Novel Visualization Approach of an Automated Image Based Glaucoma Risk Index for Intuitive Diagnosis

Jörg Meier[1], Rüdiger Bock[1], László G. Nyúl[2], Joachim Hornegger[1], Georg Michelson[3]
[1]Chair of Pattern Recognition, [3]Dept. of Ophthalmology, Univ. Erlangen, Germany;
[2]Dept. of Image Processing and Computer Graphics, University of Szeged, Hungary
joerg.meier@informatik.uni-erlangen.de

Abstract

Glaucoma is one of the most common causes for blindness worldwide. Screening is adequate to detect glaucoma at an early stage. Although it is supported by computer assisted tools no further information from former clinical studies is incorporated.

We devised a novel visualization tool that presents additional comparative image data for the diagnosis process. Automated computation of a glaucoma risk index on color fundus photographs is used to initially position an undiagnosed image in reference data. The index achieves a competitive glaucoma detection rate. The combination of the automated risk index and the new visualization technique is an important tool towards a faster and more reliable diagnosis of glaucoma.

1 Introduction

Glaucoma is one of the most common reasons for blindness in the world. Because healing of died retinal nerve fibers is not possible early detection and prevention is essential. Screening is adequate to detect abnormal changes and prevent affected persons from disease progression. Although screening is mostly supported by computer assisted tools [1], the diagnosis of glaucoma is only based on the patient's data and the experience of the physician. Data of pre-diagnosed cases from former clinical studies is available, but typically not used in the process of diagnosing a new case.

Our novel visualization tool displays additional comparative image data in relation to the current case for a more intuitive and reliable glaucoma diagnosis.

In order to improve usability and speed up diagnostic decision, we integrated an automated glaucoma risk index [2]. Initially, an undiagnosed image is positioned in the matrix according to the calculated glaucoma risk index.

2 Data

For the glaucoma risk index model we used papilla-centered color fundus photographs (Kowa non-myd, FOV 22.5°) from the Erlangen Glaucoma Registry (EGR). The gold standard for glaucoma diagnosis was set by experienced ophthalmologists with complete ophthalmological examination (ophthalmoscopy, visual field test, IOP, FDT, HRT II). The dataset consists of 100 glaucoma patients (FDT test time 67.25 ± 33.4 sec) and 100 healthy subjects. It is characterized by a mean age of 57 ± 10 years and a papilla area of 2.2 ± 0.5 mm^2; macro papillas were not included.

The reference data for the visualization is also taken from the EGR. There are 240 pre-diagnosed reference images of patients of age 55 ± 11 years and papilla sizes from 1.0 to 3.4 mm^2. The glaucoma stage is specified on a scale of 10 that has been determined by an expert.

3 Methods

As first step, the glaucoma probability score [2,3] of a given image is calculated. Preprocessing eliminates certain disease independent variations such as illumination inhomogeneities, papilla size differences and vessel structures from color fundus images (Fig 1).

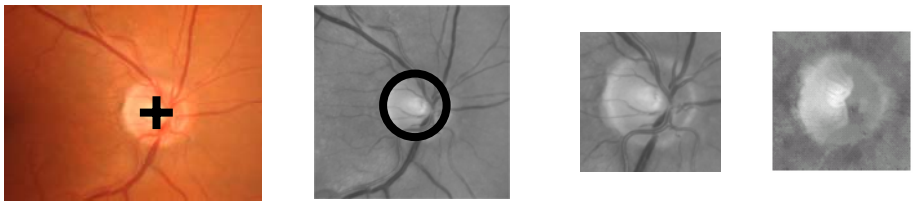

Fig 1. Preprocessing eye fundus images: Optic nerve head localization, illumination correction and rough segmentation, cropping and resizing, vessel inpainting.

Glaucomatous changes are then characterized by generic feature types such as raw pixel intensities [3] and B-spline coefficients. Compared to raw pixel intensities, spline interpolation additionally incorporates neighborhood information. B-splines of degree k = 4 showed promising results and were used in further investigations. In contrast to existing approaches these feature types are not based on segmentation measurements.

Features of each type are compressed by Principal Component Analysis (PCA) to 30 dimensions that capture at least 95% of the variance in the data. The glaucoma risk corresponds to membership probability of class “glaucoma” that is determined with a state-of-the-art probabilistic ν-Support Vector Machine. Probabilities are linearly mapped to the 10 stage glaucoma scale. Performance measurement is applied in a 10-fold cross-validation scheme.

As second step, the current observation is presented in the novel Erlangen Glaucoma Matrix that provides a context of pre-diagnosed reference images. The matrix separates different papilla sizes and varying stages of the glaucoma disease. In the matrix rows the samples range from healthy ones to advanced glaucoma cases. In the matrix columns images are ordered by the size of the optic nerve head.

The initial position of the current observation is determined by automated analysis of papilla size and the calculated glaucoma risk. In the diagnostic process the medical expert can adjust the position if necessary.

4 Results

Classification of compressed raw pixel intensities gains an accuracy of 0.83 with a specificity of 0.72 and a sensitivity of 0.94 to detect glaucomatous cases (ROC area: 0.90).

Using spline coefficient recognition a rate of 0.86 is achieved with a specificity of 0.78 and a sensitivity of 0.94 (ROC area of 0.88). The combination of both features to a common feature space and subsequent feature selection results in the superior area under the ROC curve of 0.93. Specificity slightly increased to 0.82 (sensitivity = 0.92). The different sweeps of cross-validation state a common Kappa statistic of 0.74 and thus a robust classification in case of combined features. (Fig 2).

Our proposed visualization allows evaluating an image in the context of given pre-diagnosed reference samples. Due to the two-dimensional presentation, non-disease-dependent variations (papilla size, illumination, etc.) and glaucomatous changes are shown separately. This allows studying subtle glaucoma variations separately from other deviations (Fig 3).

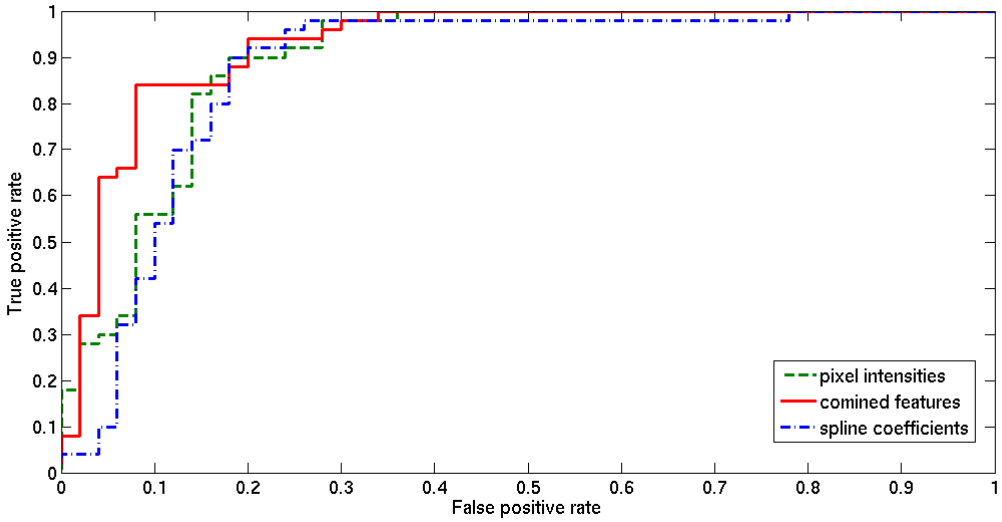

Fig 2. ROC curves of different features for detecting glaucoma from fundus photographs: Spline coefficients (ROC area: 0.88), raw pixel intensities (ROC area: 0.90), combined features (ROC area: 0.93).

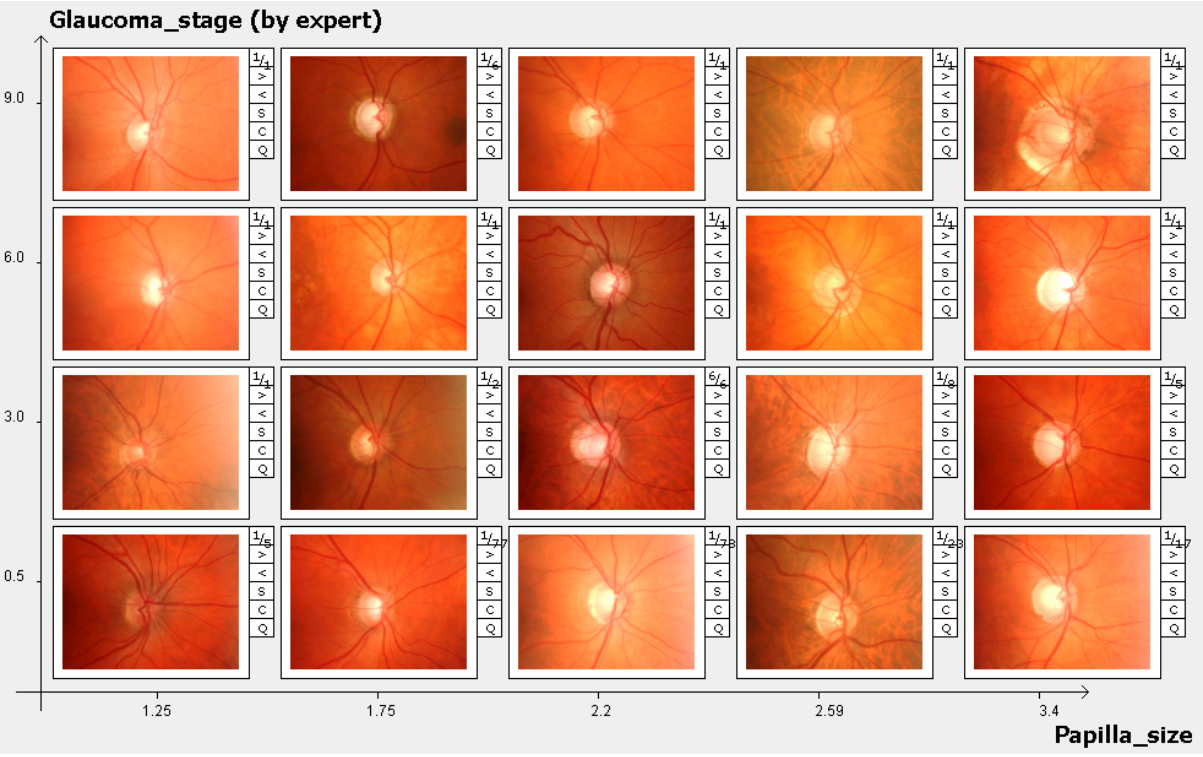

Fig 3. Erlangen Glaucoma Matrix: Visualizing fundus images in context to each other ordered by papilla size (x-axis) and glaucoma stage (y-axis). The appearance of the disease can be observed independently from the different papilla sizes.

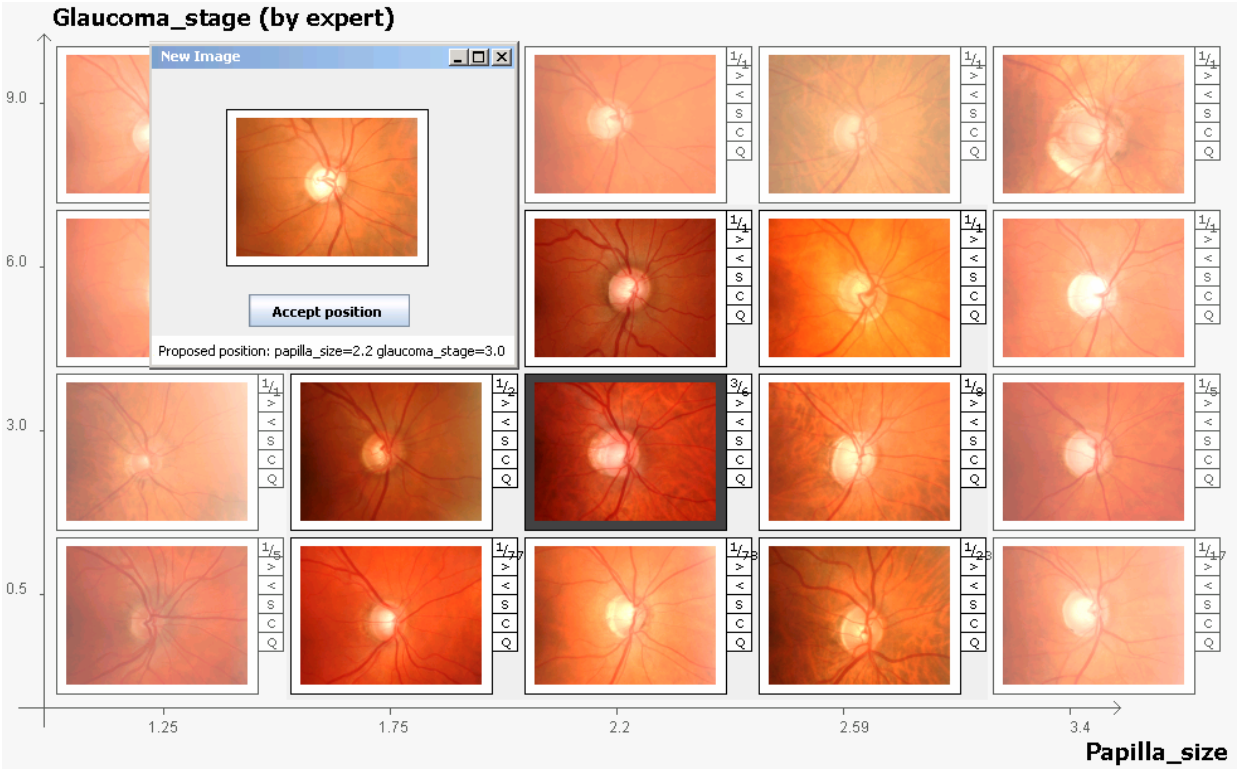

Fig 4. Showing a new image at a computed position in context of given pre-diagnosed images. The current position of the undiagnosed fundus is marked by a black frame. The initial position is proposed by automated risk index but can be changed by the user. For better comparision, the local neighborhood is highlighted.

5 Discussion

The proposed algorithm determines an automated glaucoma risk index and achieves a robust and competitive glaucoma detection rate that is adequate to initialize the position of the current observation (Fig 4). It is comparable to known methods applied to topographic papilla images [4] and does not depend on segmentation-based measurements. The glaucoma classification of a single image is difficult even for experts. Our proposed visualization provides an intuitive way for comparing similar images of the optic nerve. Thus, it supports diagnosis even in problematic cases such as macropapillas. Thus, the reliability of the physicians' diagnosis can be improved. In contrast to pure classification systems our method does not come up with a hard decision but explains the relationship to similar pre-diagnosed cases.

6 Conclusions

Our approach gives insights on glaucomatous optic nerve appearance in relation to varying papilla sizes as it shows a large diagnosed set of data separate for different glaucoma stages and papilla sizes. We have shown that fundus photography is an appropriate modality for computer-assisted glaucoma screening. The combination of an automated glaucoma risk index and this new visualization technique of a single image within reference data are considered as an important tool to confirm and speed up the diagnosis of glaucoma. It is also helpful in training glaucoma diagnostics.

Acknowledgements

The images and diagnoses used in this study were obtained from the Erlangen Glaucoma Registry. The work of R. Bock was supported by the SFB 539 subproject A4, sponsored by the German Research Foundation. The work of J. Meier was supported by a scholarship from the International Max Planck Research School Optics and Imaging. The work of L.G. Nyúl was supported by a research fellowship from the Alexander von Humboldt-Foundation.

References

[1] Hipwell, J. H.; Strachan, F.; Olson, J. A.; McHardy, K. C.; Sharp, P. F.; Forrester, J. V.: Automated detection of microaneurysms in digital red-free photographs: a diabetic retinopathy screening tool. Diabetic Medicine, 2000, 17(8), 588-594

[2] Meier, J.; Bock, R.; Michelson, G.; Nyúl, L. G.; Hornegger, J.: Effects of preprocessing eye fundus images on appearance based glaucoma classification In: 12th International Conference on Computer Analysis of Images and Patterns, CAIP. LNCS 4673, Vol. 4673/2007 Berlin, Springer 2007, pp. 165-173

[3] Bock, R.; Meier, J.; Michelson, G.; Nyúl, L. G.; Hornegger, J.: Classifying glaucoma with image-based features from fundus photographs In: 9th Annual Symposium of the German Association for Pattern Recognition, DAGM. LNCS 4713, Vol. 4713/2007 Berlin, Springer 2007, pp. 355-365

[4] Greaney, M.J., Hoffman, D.C., Garway-Heath, D.F., Nakla, M., Coleman, A.L., Caprioli, J.: Comparison of optic nerve imaging methods to distinguish normal eyes from those with glaucoma. Invest Ophthalmol Vis Sci, 2000, 43(1), 140–145